Proceedings of the 33rd Chinese Control Conference
July 28-30, 2014, Nanjing, China

Biped Walking by Elastic Potential Energy and Control Strategy

WU Botao[1,2], ZHAO Mingguo[1]
1. Department of Automation, Tsinghua University, Beijing 100084, P. R. China
E-mail: lottan3@gmail.com
2. China Satellite Maritime Tracking and Control, Jiangyin Jiangsu 214431, P. R. China

Abstract: Based on passive dynamic walking, we proposed a simple biped walking method on level ground by using elastic potential energy. To explain its working principle, the process of energy compensation is analyzed. The influences of different time delay control on the gait, walking performance, energy efficiency and stability of the model are studied by numerical simulation. Results shows that this walking method preserves the gait evolution character of passive dynamic walking and the control strategy with small time delay can improve the walking speed, while with large time delay it can improve the convergence speed from little disturbance. This research provides theoretical guidance to improve the walking performance and the robustness of the biped walking robot in practice.

Key Words: Biped walking, Elastic potential energy, Gait evolution, Control strategy

1 Introduction

At the end of the 1980's, passive dynamic walking was first proposed by McGeer [1]. The passive dynamic walker, which can walk down on a shallow slope with natural, energy-efficient and human-like gait while powered only by gravity attracts wide interest. Various passive dynamic walkers were proposed and studied [2–5]. And adding power and control to these walkers is taken as a promising way to realize human-like biped walking. Goswami proposed passivity-mimicking control laws based on the research of compass-gait model [6]. Spong [7] and Asano [8] proposed passivity-based laws and virtual passive dynamic walking method respectively. These methods actuate the robots by hip or ankle torque using the passive model as reference. Collins and Ruina built the 'Cornell biped' by using ankle push-off to provide power [9]. Asano [10], Dong Hao [11] and Xiaoyue Zhang [12] powered the robots by increasing their gravity potential energy in each step. The 'Stepper 2D' based on the 'virtual slope walking' method achieved the maximum relative speed of $4.48\ leg/s$ [11].

Besides providing power, adjusting the robot to have proper step length and period is very important, too [13]. So, we propose the method using elastic potential energy by swinging the actuated bars on the legs periodically to stretch the spring connecting the bars. This method can provide energy for the walker and adjust the gait, while preserving the properties of control simplicity and natural gait of passive dynamic walking. Numerical simulation shows that steady gait can be generated by this method. And the influence of physical and control parameters on the walking is studied.

The remainder of the paper is as follows. Section II describes the details of the model and the control strategy. The dynamics of the model are deduced using the Poincaré mapping method in Section III. In Section IV, we simplify the problem and investigate the process of energy compensation. Influences of control and physical parameters on walking gait, walking performance, energy efficiency and stability are analyzed in Section V. And Conclusions come at last in Section VI.

This work is supported by National Natural Science Foundation (NNSF) of China under Grant 61273357.

2 Description and Control Strategy

2.1 Description of the Model and Assumptions

The diagram of the planar biped robot in this paper is shown in Fig. 1. This robot consists of two stiff legs, semi-circular feet, electric motors installed at the center of mass (CoM) of each leg, two actuated bars fixed to the shaft of the motors and a spring that connects the ends of the actuated bars. In Fig. 1, the leg with lighter line stands for the stance leg and the one with heavier line stands for the swing leg.

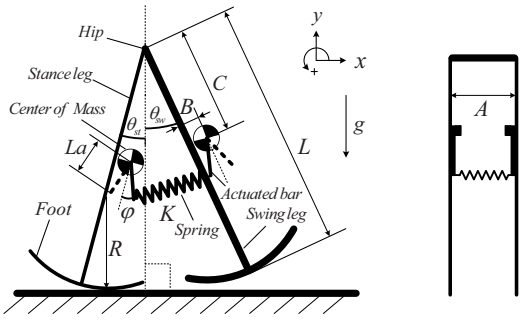

Fig. 1: Lateral and front view of the robot

Without loss of generality, we nondimensionalized the parameters, rescaling time by $\sqrt{L/g}$, mass by the mass of one leg m and length by the length of the leg L. Symbols in Fig. 1 and their values are listed in Table 1. The details of the model and assumptions are listed as follows.

Mass: All masses are lumped. The model has two mass points located at the legs and a massless pin type joint hip.

Actuation: The massless actuated bars are actuated by the motors. The bars swing from one side to the other in each step. They stop at a constant position relative to the legs. The angle between the bar and the leg is ϕ. The two stop positions are symmetrical about the legs.

Heel strike: Heel strike happens when the swing leg hits the ground. We assume this strike is instantaneous and plastic, with no slip or bounce. The motion of the robot is constrained in the sagittal plane and the foot scuffing problem of stiff-leg robots is ignored.

Table 1: Values of Parameters and Symbols

Parameter	Symbol	Value
foot radius	R	0.25
spacing between the two legs	A	0.25
CoM position (normal direction)	B	-0.01
CoM position (tangential direction)	C	-0.35
natural length of the spring	l_0	0.25
inertia of the leg	I	0.06
mass of one leg	m	1
length of the leg	L	1
spring coefficient	K	-
length of the actuated bar	La	-
angle of the actuated bar	ϕ	-
angle of the stance leg with vertical direction	θ_{st}	-
angle of the swing leg with vertical direction	θ_{sw}	-

2.2 Control Strategy

The Control strategy for the walking is that the bars swing after heel strike with different time delay τ. The bars swing back and forth during walking, from one side of the parallel lines of the leg to the other side with constant amplitude Φ during each step. The bar on the stance leg swings in the opposite direction to the one on the swing leg. Here, one step is defined as starting from the moment the swing leg leaves the ground and ending when the swing leg hits the ground. It can be divided into four parts, the first swing phase, the actuated bars' motion phase, the second swing phase and heel strike. The schematic of one step is shown in Fig. 2, the details are as follows:

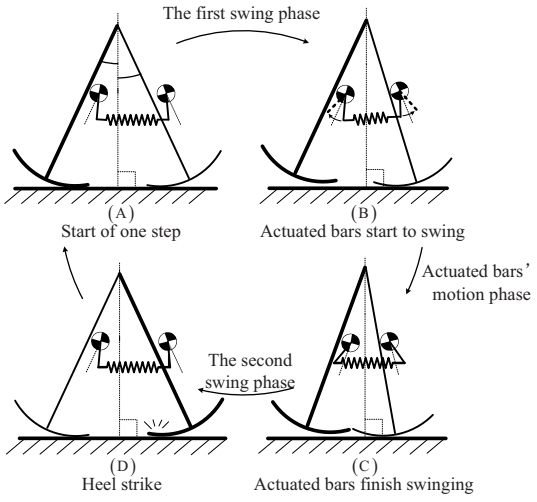

Fig. 2: Schematic of one step

(A): The moment one step starts. As shown in the figure, both legs are on the ground and the swing leg is about to leave. The ends of the bars are close to each other and the spring is not stretched.
(B): The moment just before the bars start to swing. After this instant, the bars swing to the dashed line positions. Before this instant, the position of the bars in relation to the legs remains locked.
(C): The moment just after the bars finish swing. The spring is stretched and elastic potential energy is stored into the system.
(D): The moment the swing leg hits the ground. After this instant, the swing and stance leg exchange with each other nominally. Then, the state of the model returns to (A) and a new step starts.

(A) to (B) is the first swing phase. (B) to (C) is the bars' motion phase. (C) to (D) is the second swing phase. (D) is the moment of heel strike and (A) are the moment just after it. Define the duration time from (A) to (B) as time delay τ and the duration time from (B) to (C) as the swing period T_0.

3 Dynamics

According to the process of one step, the dynamics of the robot consist of three parts, 1) the continuous dynamics which describe the motion of the first and second swing phase; 2) the continuous dynamics which describe the bars' motion phase; 3) the discrete dynamics describing the transition rule at heel strike.

To analysis the walking, define the Cartesian coordinates as shown in Fig. 1: The x-axis and y-axis are parallel to and perpendicular to the level ground respectively and the origin is at the intersection of the center of the feet with the ground.

3.1 Dynamics of the First and Second Swing Phase

Use $\boldsymbol{X}_{stcom} = (x_{st}, y_{st})^T$ and $\boldsymbol{X}_{swcom} = (x_{sw}, y_{sw})^T$ represent the CoM coordinates of the stance and swing leg respectively. We use $\boldsymbol{x} = [x_{st}, y_{st}, \theta_{st}, x_{sw}, y_{sw}, \theta_{sw}]^T$ as the state vector. According to the Newton's law, we can get the equations of the motion for the swing phase,

$$\boldsymbol{M}\ddot{\boldsymbol{x}} = \boldsymbol{F}_c + \boldsymbol{F}_g + \boldsymbol{F}_e \tag{1}$$

where $\boldsymbol{M} = diag(m, m, I, m, m, I)$, is the mass matrix, I is the inertia, $\boldsymbol{F}_c$ is the constrain force vector, $\boldsymbol{F}_g$ is the force vector of gravity, $\boldsymbol{F}_g = mg[0, -1, 0, 0, -1, 0]^T$, and $\boldsymbol{F}_e$ is the elastic force vector of the projection of the elastic force F_{eo} ($F_{eo} = K(l - l_0)$) on the motion plane by the spring, where l is the length of the spring, $l = \sqrt{\|\boldsymbol{X}_{swbar} - \boldsymbol{X}_{stbar}\|^2 + A^2}$, $\boldsymbol{X}_{swbar}$ and $\boldsymbol{X}_{stbar}$ represent the coordinates of the end of the bars on the swing leg and stance leg respectively. The coordinate of the hip is $\boldsymbol{H} = [-R \cdot \theta_{st} - (L-R) \cdot \sin(\theta_{st}), R + (L-R) \cdot \cos(\theta_{st})]^T$. Define the rotation matrix $\boldsymbol{R}_r(\theta) = \begin{bmatrix} \cos(\theta) & -\sin(\theta) \\ \sin(\theta) & \cos(\theta) \end{bmatrix}$, then

$$\begin{cases} \boldsymbol{X}_{stcom} = \boldsymbol{H} + \boldsymbol{R}_r(\theta_{st}) \cdot [B, C]^T \\ \boldsymbol{X}_{swcom} = \boldsymbol{H} + \boldsymbol{R}_r(\theta_{sw}) \cdot [B, C]^T \\ \boldsymbol{X}_{stbar} = \boldsymbol{H} + \boldsymbol{R}_r(\theta_{st}) \cdot \begin{bmatrix} La \cdot \sin(\phi) + B \\ -La \cdot \cos(\phi) + C \end{bmatrix} \\ \boldsymbol{X}_{swbar} = \boldsymbol{H} + \boldsymbol{R}_r(\theta_{sw}) \cdot \begin{bmatrix} La \cdot \sin(\phi) + B \\ -La \cdot \cos(\phi) + C \end{bmatrix} \end{cases}$$

During the first and second swing phase, the angle of the bars relative to the legs are constant. During the first phase, $\phi = -\Phi$, and during the second phase, $\phi = \Phi$. Define $\boldsymbol{n} = \boldsymbol{X}_{swbar} - \boldsymbol{X}_{stbar}$, $\boldsymbol{n}_1 = \boldsymbol{X}_{stcom} - \boldsymbol{X}_{stbar}$, $\boldsymbol{n}_2 = \boldsymbol{X}_{swcom} - \boldsymbol{X}_{swbar}$, then we have

$$\boldsymbol{F}_e = F_{eo} \cdot \frac{\|\boldsymbol{n}\|}{l} \cdot [\frac{\boldsymbol{n}^T}{\|\boldsymbol{n}\|}, \frac{\boldsymbol{n}}{\|\boldsymbol{n}\|} \times \boldsymbol{n}_1, -\frac{\boldsymbol{n}^T}{\|\boldsymbol{n}\|}, -\frac{\boldsymbol{n}}{\|\boldsymbol{n}\|} \times \boldsymbol{n}_2]^T \tag{2}$$

The operation symbol '$\times$' above is outer product.

To simplify the problem, we transform the rectangular coordinate to a generalized coordinate. Use $\boldsymbol{q} = [\theta_{st}, \theta_{sw}]^T$ as the state vector. By the principle of virtual work, we have

$$\boldsymbol{J}^T \cdot \boldsymbol{F}_c = 0 \tag{3}$$

where $\boldsymbol{J} = \partial \boldsymbol{x}/\partial \boldsymbol{q}$. By (3), eliminate $\boldsymbol{F}_c$ in (1) and have

$$\boldsymbol{J}^T \boldsymbol{M} \boldsymbol{J} \ddot{\boldsymbol{q}} + \boldsymbol{J}^T \boldsymbol{M} \dot{\boldsymbol{J}} \dot{\boldsymbol{q}} - \boldsymbol{J}^{\boldsymbol{T}} (\boldsymbol{F}_g + \boldsymbol{F}_e) = 0 \tag{4}$$

which describes the motion of the first and second swing phase.

3.2 Dynamics of Bars' Motion Phase

We assume the bars swing at a constant rate, then

$$\phi = -\Phi + 2 \cdot \frac{\Phi}{T_0} \cdot (t - \tau) \tag{5}$$

Substituted (5) into (4), we can have the dynamics of the bars swing motion. T_0 is the swing period, and $t \in [\tau, \tau + T_0]$.

3.3 Transition Rule of Heel Strike

According to the assumption at heel strike, there is an abrupt change of system states. According to the law of conservation of momentum, we have

$$\boldsymbol{M} \dot{\boldsymbol{x}}^+ - \boldsymbol{M} \dot{\boldsymbol{x}}^- = \rho \tag{6}$$

superscripts '+' and '-' represent the moment just after and before the heel strike respectively, and ρ is the momentum loss. By generalized coordinates, $\dot{\boldsymbol{x}}^+ = \boldsymbol{J}^+ \dot{\boldsymbol{q}}^+$ and $\dot{\boldsymbol{x}}^- = \boldsymbol{J}^- \dot{\boldsymbol{q}}^-$. Combining $(\boldsymbol{J}^+)^T \cdot \rho = 0$ with (6), we can get the transition rule at heel strike.

$$\dot{\boldsymbol{q}}^+ = [(\boldsymbol{J}^{sw})^T \boldsymbol{M} (\boldsymbol{J}^{sw})]^{-1} (\boldsymbol{J}^{sw})^T \boldsymbol{M} (\boldsymbol{J}^{st}) \dot{\boldsymbol{q}}^- \tag{7}$$

Equation (4), (5) and (7) describe the dynamics of walking, which we call '*Stride Function*'.

4 Simplification and Energy Compensation

4.1 Simplification

We set $\Phi = 25°$,$K = 6$, and $T_0 = 0, 0.01, 0.03, 0.05$ respectively, then use the Newton-Raphson method to search the steady gait of the model. We select θ and $\dot{\theta}$ at heel strike as the gait descriptors, and the limit cycles are shown in Fig. 3. The limit cycles shrink as T_0 increases. In practice, the bars are driven directly by electric motors, the swing period T_0 can be very short when the motors rotate fast enough. In this paper, we concentrate at the analysis of time delay τ and set the swing period $T_0 = 0$, which means the actuated bars finish the swing instantaneously and the system states have an abrupt change at bars' motion phase.

4.2 Energy Compensation

During the walking, the spring releases its elastic potential energy into the system and transforms it into the kinetic energy. We investigate the process of energy compensation by analyzing the elastic force of the spring in one step. Define $l_s = l - l_0$ as the increment of spring length. The F_{eo} with respect to l_s in one step is shown in Fig. 4.

In one step, F_{eo} changes as $C - S - A - L - O - Z - C$. The details of these key points are, C: the starting moment

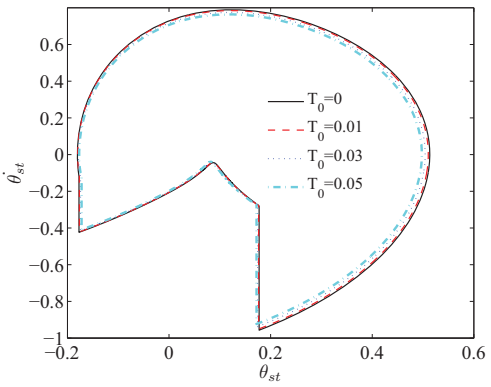

Fig. 3: Limit cycles with respect to T_0

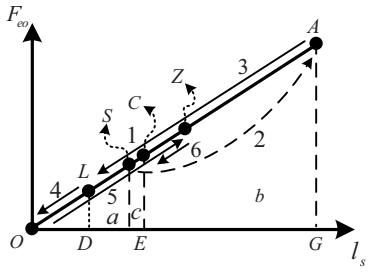

Fig. 4: F_{eo} with respect to l_s in one step

of one step, S: the moment when the actuated bars start to swing, A: the moment when the actuated bars finish swing, L: the moment when the swing and stance leg coincide in the motion plane, O: the moment when the ends of the bars coincide in the motion plane, Z: the moment when the swing leg swings to the zenith point, C: the moment when the swing leg hits the ground.

The change of F_{eo} can be divided into several stages as follows.

Stage 1: from C to S. During this stage, the swing leg leaves the ground and swings forward. F_{eo} decreases and the spring releases energy to system.

Stage 2: from S to A. The actuated bars swing to the new position, F_{eo} increases and the elastic potential energy is compensated.

Stage 3: from A to L. The swing leg swings forward to the position where it coincides with the stance leg, F_{eo} decreases and the spring keeps releasing energy to the system.

Stage 4: from L to O. The swing leg swings forward to the position where the ends of the bars coincide. F_{eo} decreases to zero.

Stage 5: from O to Z. The swing leg swings to the zenith point. F_{eo} increases and the spring absorbs energy from the system.

Stage 6: from Z to C. The swing leg retreats back. F_{eo} decreases and the spring releases energy to system again until heel strike.

The energy released into the system is larger than that absorbed from the spring, so energy is compensated by the spring. When the model walks with steady gait, the energy lost at heel strike is equal to the energy compensated.

5 Numerical Simulation

In this section, we analyze the influence of control parameters, τ and Φ, and physical parameters K and La on walking gait, walking performance, energy efficiency and stability. Several sets of parameters are chosen and we change only one parameter while keeping others constant each time. For example, we keep $\Phi = 30°$, $K = 8$ and $\tau = 0$, then change La continuously. The ranges of parameters under different sets are shown in Table 2. From the table, we can see that the ranges of parameters shrink as τ increases.

Table 2: Range of Parameters

Time delay τ	La ($\Phi = 30°$ $K = 8$)	Φ ($La = 0.13$ $K = 8$)	K ($La = 0.11$ $\Phi = 30°$)
0	$0.076 - 0.185$	$16.8 - 45.6$	$4 - 250$
0.1	$0.083 - 0.174$	$18.5 - 42.1$	$4.5 - 41.5$
0.2	$0.092 - 0.174$	$20.6 - 42.7$	$5.4 - 30.3$
0.3	$0.102 - 0.175$	$23.0 - 42.4$	$6.7 - 30.8$

5.1 Walking Gait

We use the Poincaré mapping method to analyze the walking gait, and select the system state just after heel strike as the cross section. By numerical simulation, the steady walking gait with respect to La, Φ and K at different τ are demonstrated. Under different τ, the gait evolution phenomenon that evolves from period-one gait to period-doubling gait and finally to chaos will appear as shown in Fig. 5. When $\tau = 0$, the chaos will reduce during the end part as shown in Fig. 5(a) (when La is larger than 0.17). And the reverse evolution which evolves back to period-doubling gait appears with respect to K as shown in Fig. 5(c).

5.2 Walking Performance

Human being can walk with different speed, step length and period. Based on this acknowledgement, there are three walking performance indexes we concern, the average walking speed, step length and step period. We consider 600 steps to calculate these indexes. Simulation results with respect to La, Φ and K under different τ are shown in Fig. 6.

Roughly speaking, as La or Φ or K increases the model walks with higher speed, larger step length and higher step frequency. When walking with high speed, the step length is large and the step period is small and vice versa. This is similar to human walking. Under the same parameter settings, the model walks faster with smaller time delay τ. Fast walking speed can be achieved with small time delay τ. Intuitively, the increment of spring by the actuated bars is shortened as time delay τ increases, then less energy is compensated. And by adjusting parameters, the model can walk with a wide range of speed from $0.1\ leg/s$ to $0.65\ leg/s$ and different gaits. The step length is from $0.2\ leg$ to $0.4\ leg$. The effects of adjusting La and Φ are amazingly similar to each other, which means the two parameters can replace each other when controlling the model.

5.3 Energy Efficiency

We use the specific cost of transport c_t to measure the energy efficiency of the model [14] and c_t is defined as

$$c_t = \frac{Energy\ Used}{Weight \cdot Distance\ travelled} \tag{8}$$

Numerical results are shown in Fig. 7. Under different τ, the minimum c_ts are approximate to each other and the minimum value is as low as 0.0251, which can be well matched with other energy-efficient biped robots introduced in [14]. With smaller τ, the model walks with higher speed and c_t gets higher. And it is more energy efficient to walk slowly.

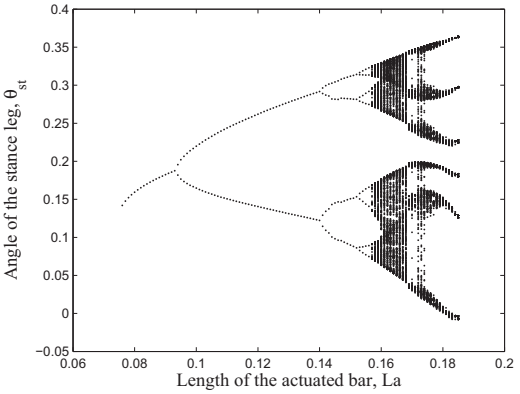

(a) Gait evolution with respect to La, $\tau = 0$

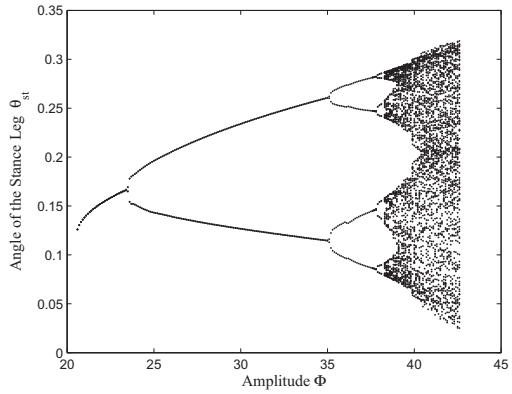

(b) Gait evolution with respect to Φ, $\tau = 0.2$

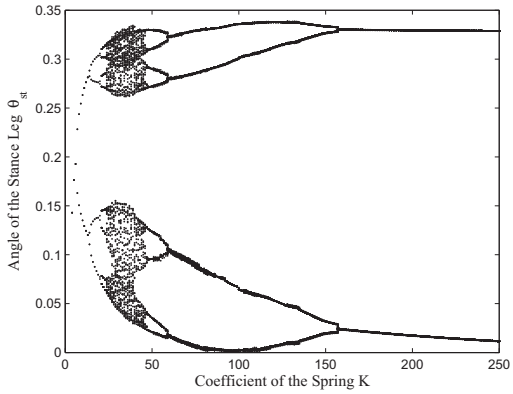

(c) Gait evolution with respect to K, $\tau = 0$

Fig. 5: Diagrams of gait descriptor evolution with respect to La, Φ and K under different τ. (a) $\Phi = 30°$ and $K = 8$, $0.076 \leq La \leq 0.185$, when $\tau = 0$. (b) $La = 0.13$ and $K = 8$, $20.6° \leq \Phi \leq 42.7°$, when $\tau = 0.2$. (c) $La = 0.11$ and $\Phi = 30°$, $4 \leq K \leq 250$, when $\tau = 0$.

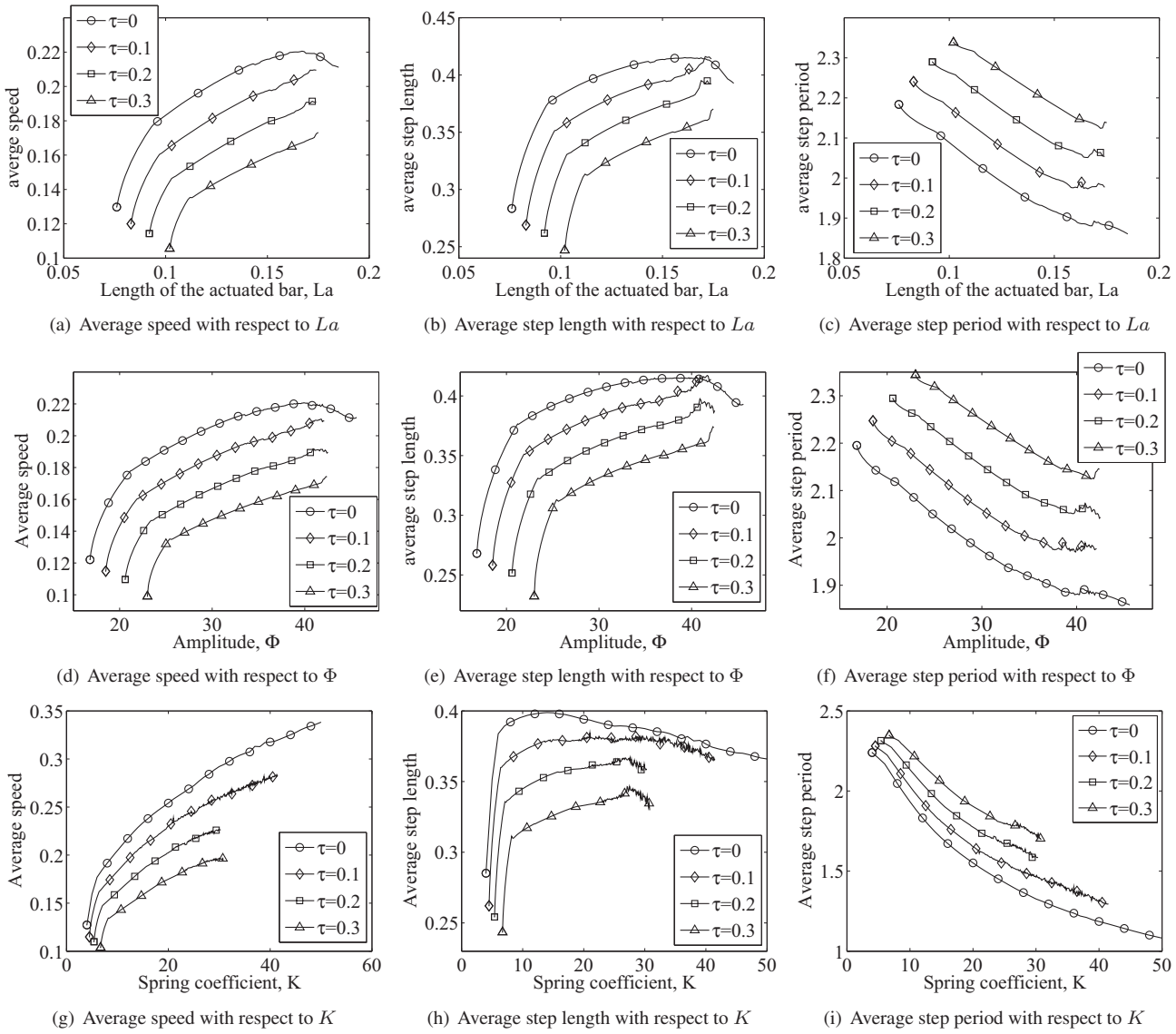

(a) Average speed with respect to La (b) Average step length with respect to La (c) Average step period with respect to La

(d) Average speed with respect to Φ (e) Average step length with respect to Φ (f) Average step period with respect to Φ

(g) Average speed with respect to K (h) Average step length with respect to K (i) Average step period with respect to K

Fig. 6: Diagrams of average speed, step length and step period with respect to La, Φ and K under different time delay τ. For (a), (b) and (c), $\Phi = 30^\circ$ and $K = 8$. For (d), (e) and (f), $La = 0.13$ and $K = 8$. For (g), (h) and (i), $La = 0.11$ and $\Phi = 30^\circ$. $\tau = 0, 0.1, 0.2, 0.3$ respectively.

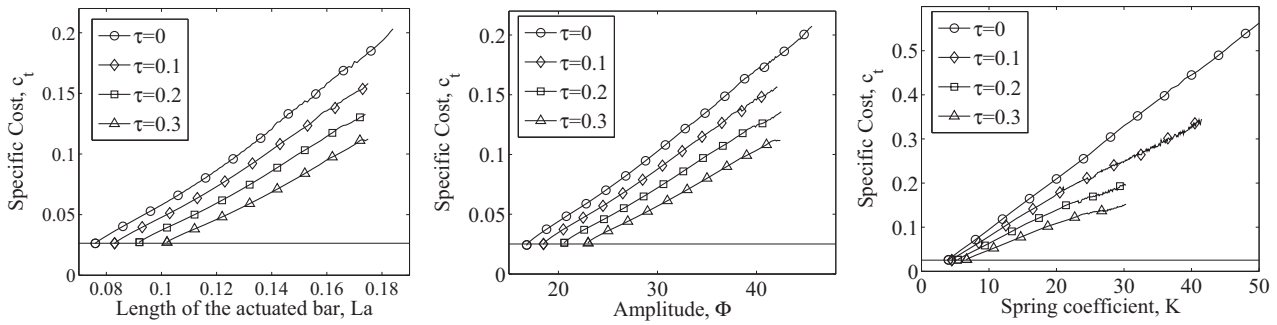

(a) c_t with respect to La (b) c_t with respect to Φ (c) c_t with respect to K

Fig. 7: The c_t with respect to La, Φ and K under different τ. (a) $\Phi = 30^\circ$ and $K = 8$. (b) $La = 0.13$ and $K = 8$. (c) $La = 0.11$ and $\Phi = 30^\circ$.

5.4 Local Stability

The maximum Floquet multiplier (MFM) is used to investigate the local stability here. The Floquet multiplier is the eigenvalue of the Jacobian matrix at the fixed point. It indicates whether the fixed point is stable and how fast will the system state converge when there is small deviation from the fixed point. For linear system, if all of the Floquet multipliers are in the unit circle, the fixed point is stable and the system state will recover with small deviation. The smaller the maximum Floquet multiplier is, the faster will the system state converges. Otherwise, small deviation will cause even larger deviation and the system state will deviate from the fixed point. The period-one gait is investigated here. The MFMs with respect to La, Φ and K under different τ are shown in Fig. 8. Generally, when τ is larger than 0, the MFM is smaller and the local stability of the model is stronger.

6 Conclusions

In this paper, a method using elastic potential energy as power source is proposed to actuate a biped robot. The dynamics are deduced and by analyzing the process of energy compensation, it shows that energy is compensated effectively in the form of elastic potential energy. By numerical simulation, we show that steady gait is generated by this method. Special gait that has reverse evolution is found. The influences of control and physical parameters on walking performance, energy efficiency and local stability are analyzed. And a wide range of speed and various gaits can be achieved under this method. When building a robot, an impact sensor to detect the heel strike is needed. With time delay control, the request for time precision is lower and this can make the robot more robust in practice.

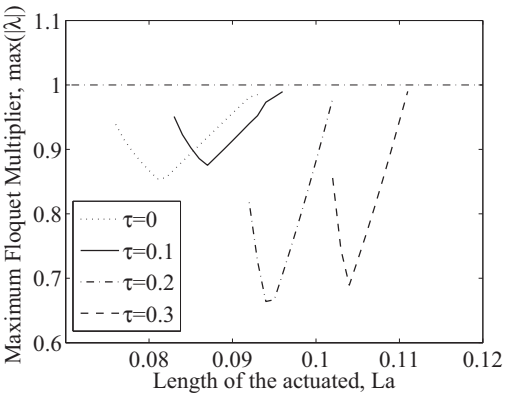

(a) MFMs with respect to La

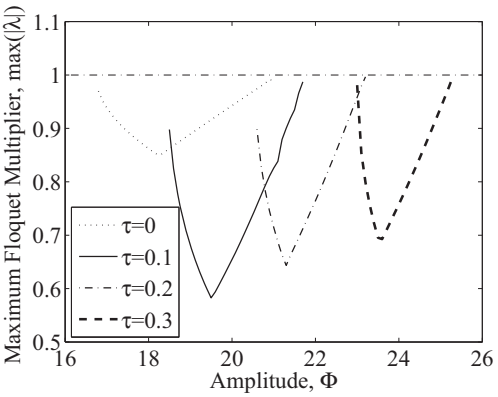

(b) MFMs with respect to Φ

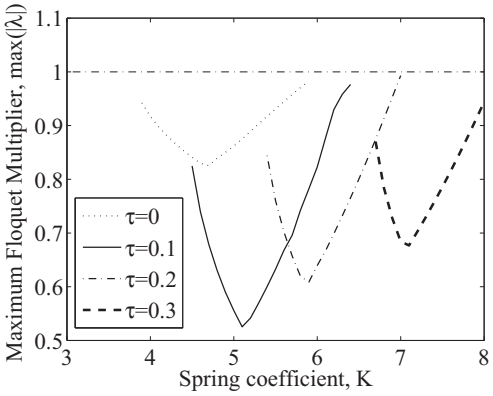

(c) MFMs with respect to K

Fig. 8: The MFMs of period-one gait with respect to La, Φ and K under different τ. (a) $\Phi = 30^\circ$ and $K = 8$. (b) $La = 0.13$ and $K = 8$. (c) $La = 0.11$ and $\Phi = 30^\circ$.

References

[1] T. McGeer, Passive dynamic walking, International Journal of Robotics Research, 9(2):62-82, Apr. 1990.

[2] A. Goswami, B. Espiau, A. Keramane, A study of the passive gait of a compass-like biped robot: symmetry and chaos, International Journal of Robotics Research, 17(12):1282-1301, 1998.

[3] M. Garcia, A. Catterjee, A. Ruina, M. J. Coleman, The simplest walking model: stability, complexity, and scaling, ASME J. Biomech. Eng., 120(2):281-288, 1998.

[4] T. McGeer, Passive walking with knees, Robotics and Automation, 1990. Proceedings., 1990 IEEE International Conference on. IEEE, 1990: 1640-1645.

[5] M. Wisse, Essentials of dynamic walking; Analysis and design of two-legged robots, Delft University, 2004.

[6] A. Goswami, B. Espiau, A. Keramane, Limit cycles in a passive compass gait biped and passivity-mimicking control laws, Autonomous Robots, 4(3):273-286, 1997.

[7] M. W. Spong, Passivity-based control of the compass gait biped, In Proc. of the IFAC world congress, 1999:19-23.

[8] F. Asano, M. Yamakita, K. Furuta, Virtual passive dynamic walking and energy-based control laws, In Proc. of IEEE/RSJ International Conference onIntelligent Robots and Systems (IROS), 2000:1149-1154.

[9] S. H. Collins, A. Ruina. A Bipedal Walking Robot with Efficient and Human-Like Gait. In Proc. of IEEE International Conference on Robotics and Automation, 2005:1983-1988.

[10] F. Asano, Z.-W. Luo, Energy-efficient and high-speed dynamic biped locomotion based on principle of parametric excitation. IEEE Transaction on Robotics, 24(6):1289-1301, 2008.

[11] H. Dong, M. Zhao, N. Zhang, High-speed and Energy-efficient Biped Locomotion based on Virtual Slope Walking. Autonomous Robot, 30(2):199-216, 2011.

[12] X. Zhang and M. Zhao, Analysis of a biped powered walking model based on potential energy compensation, In Proc. of the IEEE/ROBIO International Conference on Robotics and Biomimetics, 2009:1445-1450.

[13] M. Zhao, B. Hu, Analysis of the disturbance rejection ability of a passive dynamic walker with hip spring, Robotics and Biomimetics (ROBIO), 2012 IEEE International Conference on. IEEE, 2012: 54-60.

[14] S. H. Collins, A. Ruina, R. Tedrake, and M. Wisse, Efficient bipedal robots based on passive-dynamic walkers, Science, 307(5712):1082-1085, 2005.